1

Control of Electronic Property of C_{60} Fullerene via Polymerization

Nobuyuki Aoki

Chiba University, Graduate School of Science and Engineering, Department of Materials Science, 1-33 Yayoi, Inage, Chiba 263-8522, Japan

1.1 Introduction

1.1.1 History of Polymerization of C_{60} Fullerene

Fullerenes, the spherical cage molecules composed of carbon atoms, were discovered by Kuroto and Smalley coworkers in 1985 [1]. After the development of a large-scale synthesis method by Kraetschmer et al. in 1990 [2], they became usable not only in vacuum but also in atmospheric conditions. C_{60} is the most popular molecule in the fullerenes composed of 60 carbon atoms as shown in Figure 1.1a. It has semiconductor characteristics having a bandgap. The experimental values have been shown as typically 1.5–1.8 eV for the highest occupied molecular orbital–lowest unoccupied molecular orbital (HOMO–LUMO) gap [3, 4]; however, the value varies within the range of 1.43–2.35. The electrical properties of fullerene are based on the bandgap. It shows n-type semiconductor characteristics; the activation energy is less than half of the bandgap and is close to the half value only at high temperatures. At around room temperature, the activation energy is in the range of 100–200 meV, which relates to activation from the donner-like state within the optical gap [5]. The transport properties are strongly affected also by the orientation state of the crystalline fullerene. On decreasing the temperature from room temperature, the first kink of the conductivity is observed at around 260 K related to the restriction of the orientation angle of rotation of C_{60} molecules [6]. The second kink at 90 K relates to the glass transition of the orientation angle.

The conductivity drastically falls by several orders of magnitude, mostly becoming insulating due to absorption of oxygen molecules [7]. This is due to the formation of deep level trap sites lying 0.7 eV below the bottom of the conduction band. Therefore, most of the transport measurements of the semiconducting properties are done in vacuum conditions. An inert atmosphere such as argon, nitrogen, or helium also helps maintain the conductivity. If the sample was exposed in air once, heating at 160–180 °C in vacuum is necessary to recover the conductivity by desorbing oxygen from the thin film of fullerene [8].

Molecular Technology: Materials Innovation, Volume 3, First Edition.
Edited by Hisashi Yamamoto and Takashi Kato.

Crystalline C_{60} fullerene exhibits face centred cubic (fcc) structure due to van der Waals interaction. Intermolecular interactions change the electrical and optical properties. A possibility of intermolecular coupling was observed first by photo-irradiation using laser light [9]. UV–visible light illumination read the photopolymerization of the C_{60} molecules in oxygen-free condition since oxygen hinders the reaction by forming photoexcited triplets [10]. Such a process occurs only above 260 K since a random orientation of the rotation is essential for the polymerization process.

Photo-transformation takes place by [2+2] cycloaddition reaction mechanism [11], where faced double molecular bonds are broken and a four-member ring is formed as shown in Figure 1.1a.

Such a dimer structure is called "dumbbell type" polymerization. For the occurrence of the polymerization reaction, the following requirements can be summarized:

(i) The C_{60} molecules should be situated close enough to each other (an application of pressure assists this situation).
(ii) They must be rotating freely.
(iii) Their double bonds must be faced in parallel.
(iv) Certain external energy that opens the double bond must be applied (photoexcitation, thermal agitation, plasma, electron beam [EB] absorption, pressure application, etc.).
(v) A four-atom carbon ring is formed.

After forming the intermolecular bonding, the mean intermolecular length, typically 1.0 nm in fcc structure, shortens to 0.01–0.03 nm. And then, the free rotation of the molecule stops, and solubility in polar organic solvents such as toluene, xylene, hexane, and so on is lost. For the photochemical reaction between C_{60} molecules, the following reaction scheme is proposed [11]. Although the [2+2] cycloaddition of neutral C_{60} molecules is thermally forbidden due to the Woodward–Hoffmann rules, this type of reaction is photochemically allowed between an excited and a ground state molecule. The interaction of the singly occupied π^*-orbital of the photoexcited molecule with the unoccupied π^*-orbital of the ground state molecule, as well as the interaction of the singly and doubly occupied π-orbitals gives rise to a symmetrically allowed and energetically favorable transition state. The simplified orbital interactions of two C=C double

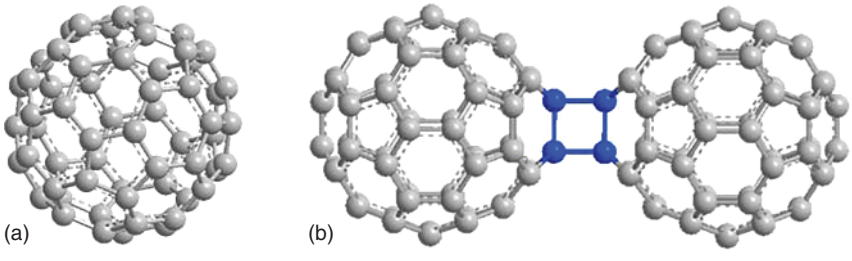

Figure 1.1 Structural model of a C_{60} fullerene molecule (a) and a fullerene dimer having a dumbbell structure (b).

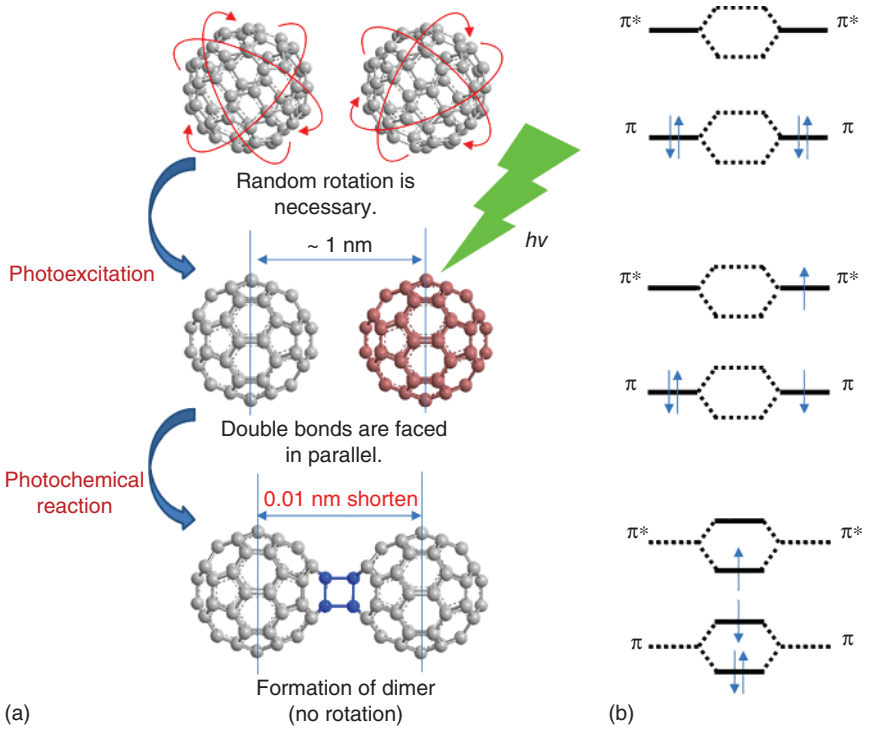

Figure 1.2 Schematic of the photochemical reaction (a) and energy diagrams of frontier orbital interactions of reactants in [2+2] cycloaddition reactions (b).

bonds are illustrated in Figure 1.2. Such a polymerization process in a solid or a thin film of C_{60} can also take place by other means: application of high pressure at high temperature, intercalation of alkali metals, plasma treatment, EB irradiation, and so on. If a negative ion reacts with a neutral ground state molecule, the interaction of the singly occupied and the vacant π*-orbitals results in a lower energy transition state, similarly to the photochemical mechanism.

For the intermolecular bond formation, two types of possibilities are proposed. In one configuration, the two C atoms shared by the two adjacent hexagons in a C_{60} are covalently bonded to the C atoms that are shared by the two hexagons in the adjacent C_{60} (66/66 bond); in another, the two C atoms shared by a hexagon and a pentagon in a C_{60} are bonded to the adjacent C_{60} (66/65 bond) shown in Figure 1.3b. It is known that the 66/66 bond is more stable thermodynamically than the 66/65 one; therefore, the 66/65 one must be a very rare case [12, 13]. However, existence of a C_{60} polymer composed of 66/65 bonds (Figure 1.3b) is the only model to explain the metallic property of the polymer having a two-dimensional rhombohedral (rh) structure realized by high temperature and high pressure application [14].

Hence, we can control the electrical properties of C_{60} fullerene depending on the polymerized structure. In this chapter, after showing the basic electrical properties of a pristine C_{60} fullerene, various kinds of polymerization regimes and the electrical properties will be introduced.

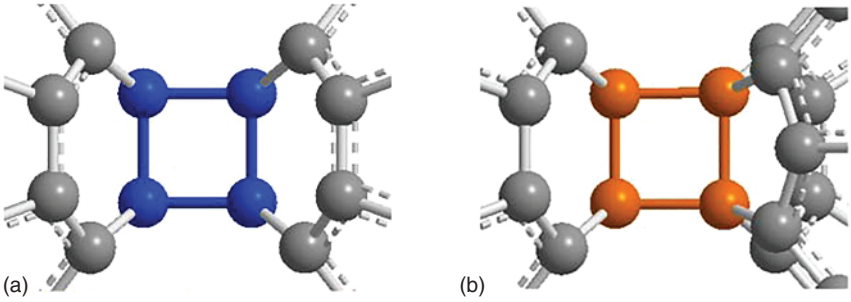

Figure 1.3 (a) 66/66 and (b) 66/65 bonding structures.

1.1.2 Electronic Property of Pristine C_{60} and n-Type FET Action

The first C_{60} field effect transistor (FET) was reported by Paloheimo et al. [15] in 1993 and developed by Haddon et al. [16] in 1995. They clarified that C_{60} FET works as an n-type transistor and exhibits fairly good carrier mobility around 0.1 cm^2 V^{-1} s^{-1}. The highest mobility is more than 10 cm^2 V^{-1} s^{-1} as reported by Li et al. in 2012 [17]. The properties are severely dependent on the environment. After being exposed in air or oxygen, the conductance suddenly drops and it becomes almost insulating [7]. Therefore, most of the transport experiments are performed in vacuum conditions. The conductance also depends on temperature, so that there might be a large amount of charge trapping states, in other words donor-like states, in the pseudo gap of C_{60} FET [18]. In general, these states usually come from structural disorders at crystalline defect or grain boundary, as well as from polaronic disorders introduced by guest impurities. The latter would be an effect of oxygen adsorption, by which the conductance decreases drastically. Therefore, transport measurements of a C_{60} FET require an oxygen-free environment such as vacuum or inert gas, or covering by a passivation layer [19]. Figure 1.4 shows typical current–voltage (I–V) curve and transfer curves of a C_{60} thin film FET. The FET structure is fabricated on a SiO_2 layer of heavily doped Si wafer. The electrical contacts are performed by Au. The channel length and width are 5 and 100 μm, respectively. The field effect mobility, μ, in the low field region can be estimated from the following equation [20]:

$$\mu = \frac{I_D L}{C_{ox} W \left\{ V_{DS}(V_{GS}\text{-}V_T)\text{-}\frac{1}{2}{V_{DS}}^2 \right\}}$$

where I_D is the drain current, L is the channel length, W is the channel width, C_{OX} is the gate capacitance of oxide layer, V_{DS} is the drain voltage, V_{GS} is the gate voltage, and V_T is the threshold voltage. Considering the threshold voltage to be 15 V, the mobility is estimated as 0.1 cm^2 V^{-1} s^{-1}.

The temperature dependence of a C_{60} FET shows nearest neighbor hopping, which depends on T^{-1} at temperatures lower than room temperature. However, below 100 K, variable range hopping (VRH) has been observed in the conductance of C_{60} FET [21]. In this transport regime, the conductance drops with decreasing temperature depending on the following relation:

$$\sigma \propto \exp(-T^{-1/4})$$

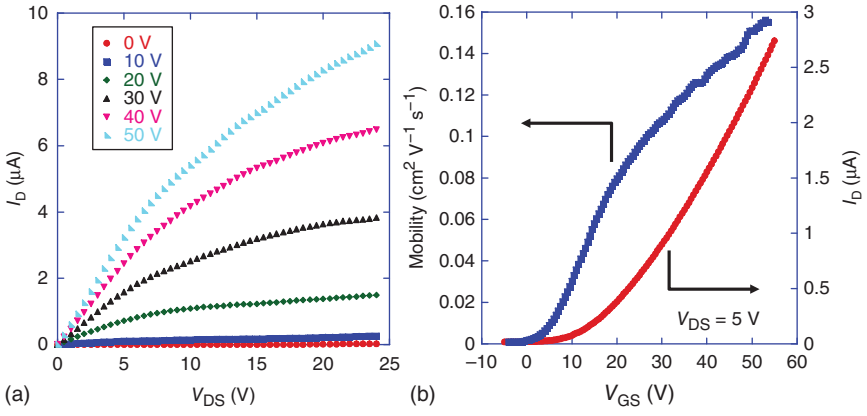

Figure 1.4 Typical transistor curves of a C_{60} thin film FET (a). Transfer curve and estimated mobility (b).

This relationship indicates that the transport is three dimensional in the thin film of C_{60} since the suffix of T can be obtained from $1/(d+1)$ where d is the dimensionality of electron transport of the system. In general, conduction carriers in VRH can transport by hopping among electronic states at Fermi level (E_F), which enables us to estimate the density of charge trapping states in the pseudo gap of C_{60} thin film.

1.2 Polymerization of C_{60} Fullerene

1.2.1 Photo-irradiation

Photopolymerization of C_{60} thin film under visible or UV irradiation was confirmed first by Rao et al. in 1993 [9]. The reaction was confirmed using UV–visible light from a Hg arc lamp or an Ar ion laser having a wavelength of 488 nm on C_{60} thin films of thickness of several hundred nanometers on a Si substrate. One typical evidence of the photopolymerization is a peak shift of $A_g(2)$ mode in the Raman scattering spectrum, which corresponds to the pentagonal pinch mode of the C_{60} molecule [22]. The peak occurs at 1469 cm^{-1} before the light irradiation and shifts to 1460 cm^{-1} after the irradiation. The mechanism of photo-transformation is based on [2+2] cycloaddition reaction [11]. A 1D polymer chain of C_{60} molecules having an orthorhombic crystal structure is proposed for this photopolymer. The polymerization reaction occurs within a temperature range between 260 and 400 K without applying pressure. The lower limit is due to the necessity of free rotation of C_{60} molecules. On the other hand, the upper limit is restricted by a depolymerization process due to an increase in thermal vibrations. Therefore, the intermolecular bonding is broken by heating to more than 473 K so that the photopolymer reversibly returns to the monomer [23]. The activation energy for the depolymerization process is approximately 1.25 eV [22]. For the photopolymerization, light having photon energy greater than the bandgap energy of the C_{60} molecules is necessary. Existence of long

chains of more than 20 C_{60} molecules was confirmed by laser desorption mass spectrum from C_{60} thin film after sufficient UV–visible light irradiation [9]. Figure 1.5a shows typical Raman shift peaks of $A_g(2)$ mode of a C_{60} thin film. The peak occurs at 1469 cm^{-1} before irradiation; however, it shifts to 1460 cm^{-1} after green laser irradiation for 10 minutes. On the other hand, no significant peak shift can be confirmed; Raman peaks of a solid single crystal before and after laser light irradiation are shown in Figure 1.5b. In the case of the thin film, the peak shift occurs very easily even during the irradiation for Raman spectroscopy. In other words, it is very difficult to obtain a Raman peak of the pristine C_{60} thin film at 1469 cm^{-1}. In the case of photopolymerization, it is basically difficult to obtain long chain polymers. The polymer chain is mainly of short-range oligomers such as dimer or tetramers. The $A_g(2)$ peak position shifts to further lower frequency through progress of the polymerization reaction of C_{60}. The shoulder at 1453 cm^{-1} can be assumed as the peak corresponding to a polymer higher than a dimer (e.g. trimer). Generally, no long-range order can

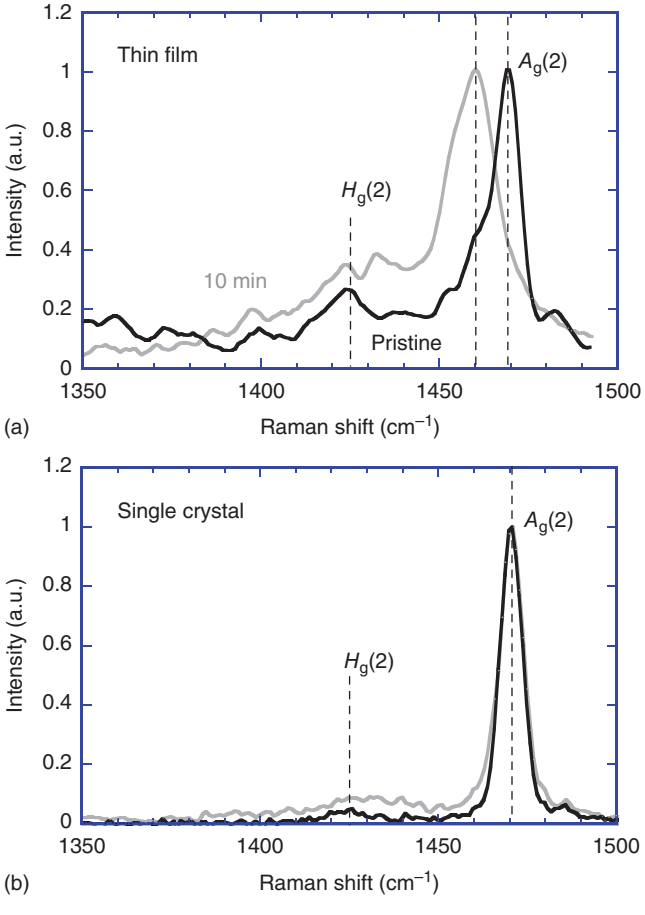

Figure 1.5 Typical peak shifts of $A_g(2)$ mode before (black) and after (gray) laser irradiation of a thin film (a) and a single crystal (b).

be observed in the photopolymer of the thin film unlike in pressure-induced polymerization.

A C_{60} photopolymer still shows semiconducting electric property [24]. The evolution of gate voltage dependences of a C_{60} thin film FET with laser light irradiation is shown in Figure 1.6. The FET sample has a C_{60} thin film of 50 nm thickness and the electric contacts occur underneath the thin film, forming a bottom contact structure. In the case of such an FET, the ON current of the FET decreases with increasing dose of the green laser beam. Consequently, a decrease in the mobility was confirmed. In this sample structure, since a laser beam was irradiated from the top of the thin film, photopolymerization takes place from the surface of the film. Therefore, at the bottom of the film, the molecules must be polymerized partially and then such a disorder affects the decrease of the mobility.

Basically, polymerization by photo-irradiation is never perfect in the bulk region of a C_{60} thin film and a solid of a single crystal since the dimerization of two C_{60} molecules hinders successive, long-chained, photo-polymerization. However, polymerization at the surface of a thin film shows different behavior. 2D-rhombohedral rinks of C_{60} molecules were confirmed on a thin film after irradiation with UV–visible light (photon energy: 2–4 eV, light intensity: 3–4 W cm^{-2}) for 400 hours at room temperature in vacuum [25]. The resistivity was of the order of 10^3 Ω cm. More recently, we also observed the formation of two-dimensional polymer films synthesized on a C_{60} thin film after sufficient irradiation with optical vortex (OV) laser light [26]. Figure 1.7 shows the atomic force microscope image of the surface of the irradiated region. A film having a thickness of 1 nm can be confirmed on the grains in a C_{60} thin film. The coverage on the surface depends on the dose of the laser light. Such a film reminds us of a 2D polymer phase having te- and rh-structures. When we placed two electrodes on the irradiated region after the irradiation, we confirmed no gate voltage dependence of current through the sample, which suggested a metallic property (sufficient amount of carriers exist in a sample without applying a gate voltage). Surprisingly, the current can be confirmed even in air since a C_{60} thin film becomes insulating immediately after being exposed in air. The mechanism is still under discussion; however, the experimental results suggest that even

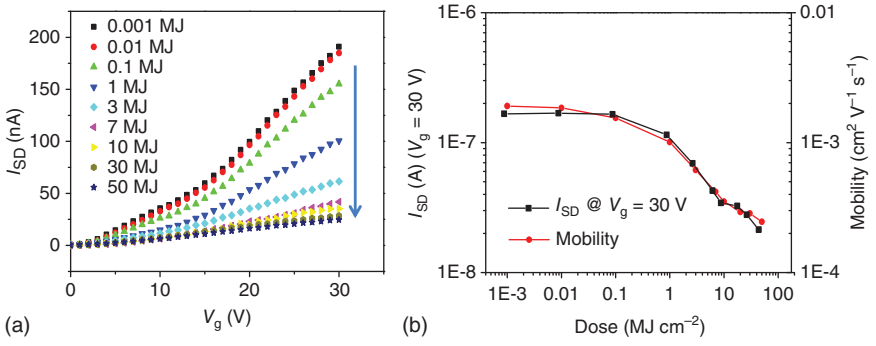

Figure 1.6 Typical effect of photopolymerization on transfer curves of a C_{60} FET (a). The mobility decreases as well as the ON current incrementing the dose (b).

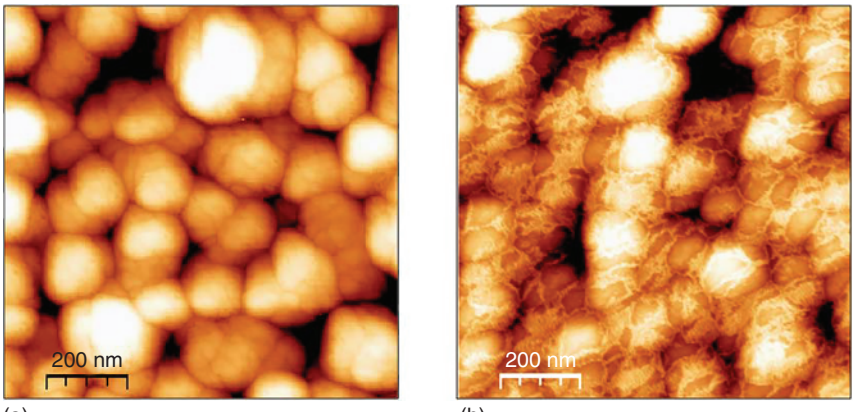

Figure 1.7 AFM image of C_{60} thin film out of (a) and within (b) the OV irradiated region.

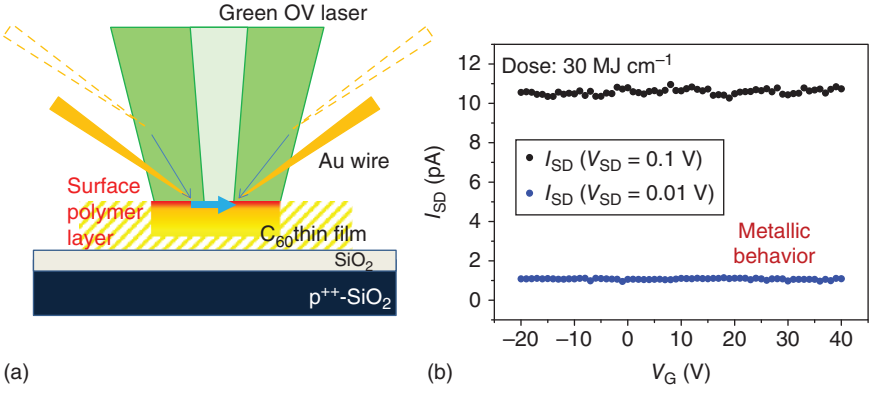

Figure 1.8 Schematic view of OV irradiation on a C_{60} thin film and the electrical measurement within the irradiated region using Au wires after the irradiation (a). Two terminal transfer curves at different bias voltages (b). No gate voltage dependence was observed.

photo-polymerization may provide a metallic 2D polymer at the surface of thin films after sufficient irradiation (Figure 1.8).

1.2.2 Doping Effect Using Alkali Metal and Superconductivity

Doping into C_{60} fullerene molecules is accompanied by 3-D intercalation of alkali, alkali earth, and rare earth metals forming compounds [27]. Owing to the intercalation, electrons can be delivered into the unoccupied band whose lattice can store up to six electrons, without forming the chemical bond unlike the conventional covalently-bonded semiconductors such as Si. A_XC_{60}, where X can be changed from one to six in stoichiometric ratio, which has different characteristics depending on the number of X. A_1C_{60} and A_3C_{60} show metallic property while the other structures have semiconducting property. Especially, A_3C_{60} compound is well known to exhibit superconducting property at low

temperature. The critical temperatures of K_3C_{60} and Rb_3C_{60} are 19.8 and 30.2 K at normal pressure, respectively [28]. On the other hand, the A_1C_{60} (A = K, Rb, or Cs) compound shows different behavior. It is reported that the crystal has an orthorhombic structure and the C_{60} molecules have a covalent bond with each other one dimensionally. X-ray diffraction pattern of the material shows good agreement with the calculated atomic position of orthorhombic phase with [2+2] cycloaddition below 350 K [29]. The mechanism of the formation of intermolecular bonds is explained by ion-induced [2+2] cycloaddition [30]. Such a structure can be obtained via the following process; alkali ions such as K^+, Rb^+, and Cs^+, which are larger than the tetrahedral space of fcc C_{60} crystal, can form a doped structure with one ion per octahedral position. The compound takes a NaCl (fcc) structure at high temperatures (e.g. more than 420 K for KC_{60}). It can be balanced by Coulomb interaction between A^+ and C_{60} and a slight distortion of the crystal. The structure undergoes first-order phase transition into a body-centered orthorhombic structure. The structure is formed by the distortion of the fcc lattice without diffusing the metal ion out from the crystal. And then, [2+2] cycloaddition takes place and the one-dimensional polymer is formed. This polymerization scheme is basically similar to a process in high-pressure application; however, the dimensionality of the polymerized crystal is different. The fcc structure is not stable at room temperature and transits into an orthorhombic polymer phase. A single crystal of $(KC_{60})_N$ was grown; it was a few millimeters long and the degree of polymerization exceeded 100 000 [31]. At low temperatures such as liquid nitrogen temperature, the crystal forms a superstructure by dimerization within the 1D crystal.

1.2.3 High-Pressure and High-Temperature Application

As mentioned above, depolymerization process occurs at more than 200 °C in normal pressure; however, application of pressure with heating brings about the other phases of polymerization. Iwasa et al. reported the first polymerization with a rhombohedral (rh-phase) structure in 1994 [32]. They heated C_{60} crystals up to 1073 K by applying a pressure of 4–8 GPa. The other phases, orthorhombic (or-phase) and tetragonal (te-phase), were confirmed in latter experiments [33]. Their crystalline structures have been determined by X-ray diffraction patterns. Successive transition was observed from fcc structure to 1D- (or-phase) or 2D- (te- and rh-phase) polymerized phase by increasing the temperature and applying pressure. A mixture of rh- and te- phases is formed at 2–4 GPa and 673–1073 K, and a pure rh-phase at 4–8 GPa and the same temperatures [34]. By applying pressure, the intermolecular distance is decreased and the regularity of rotation angle is restricted; therefore, the crystalline structure changes from fcc to simple cubic (sc) phase, which is a more restricted structure. Since such a restriction of rotation angle hinders the formation of intermolecular bond by [2+2] cycloaddition process, polymerization does not progress in the sc phase. However, by increasing the temperature, the transition in the sc phase is suppressed and it returns to the fcc phase again, and then the angular disorder of the rotation also reappears. Therefore, higher order polymerization such as the te- and rh-phase can be obtained at high pressure and high temperature conditions.

Typically, more than 5 GPa and 973 K are necessary for the formation of the rh-phase [34].

Since rh-polymer phase has 2D and a hexagonal symmetry, the crystal exhibits a hexagonal or triangular shape. On the other hand, the te-phase polymer shows a square-shaped crystal. Makarova et al. show the transport properties of each polymer [35]. Both te- and rh-polymers show semiconducting characteristics; the resistance increases with decreasing temperature. However, an rh-phase sample synthesized at 7–8 GPa and 973–1073 K shows metallic property; the resistance decreases with decreasing temperature (Figure 1.9).

Okada and Oshiyama showed the results of the first principles calculation of band structures of the rh-polymer phase [36], which is composed of normal 66/66 bonds and has a bandgap at the Fermi energy as shown in Figure 1.10. Therefore, there is still room for discussion on the mechanism; however, the only clear mechanism is that of an rh-phase polymer having 66/65 bonds. Metallic band structures are suggested in both cases of ABA and ABC staking of rh-phase polymer layers of 66/65 bonds.

If a C_{60} crystal is heated at over 1273 K in 5 GPa, the cages of C_{60} molecules are broken and become amorphous carbon [37].

The peak shifts of $A_g(2)$ mode in Raman spectrum in the different polymer structures are summarized by Rao et al. [38]. However, the suggested peak assignments of the Raman shift in each phase include ambiguity. It is difficult to obtain a pure sample having a single polymer phase, as multiple phases are usually involved in it. Therefore, in the early stages of the experiments, mixed peaks were occasionally misassigned in the spectrum. The most reliable experimental result shown by Meletov et al. is that a peak wave number of $A_g(2)$ mode in pure rh-phase of C_{60} crystal appears at 1408 cm^{-1} as shown in Figure 1.11 [39]. They prepared the single crystal of rh-phase sample by applying a high pressure of 5 GPa at 773 K. By heat treatment at more than 523 K for 0.5 hour, the peak height at 1408 cm^{-1} decreased and then peaks corresponding to the 2D-te-phase and the 1D-or-phase began to appear as shown in Figure 1.11. After thermal treatment at 548 K for 0.5 hour, these peaks also disappeared and only a peak of 1469 cm^{-1} corresponding to the C_{60} monomer finally remained. Even at

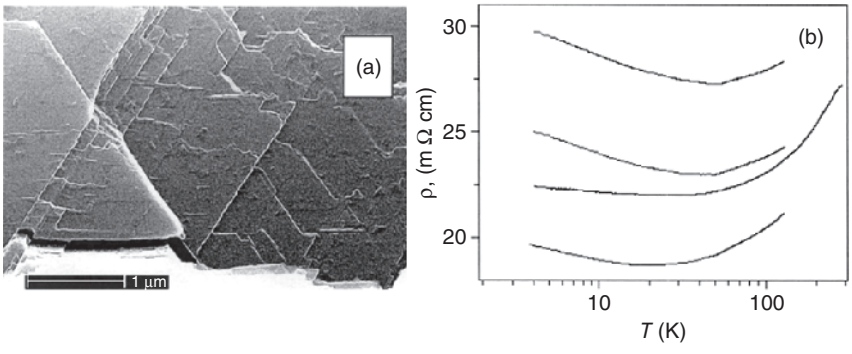

Figure 1.9 Scanning electron microscope image of polymeric C_{60} crystal having rh-phase (a) and temperature dependences of the resistivity (b) [35].

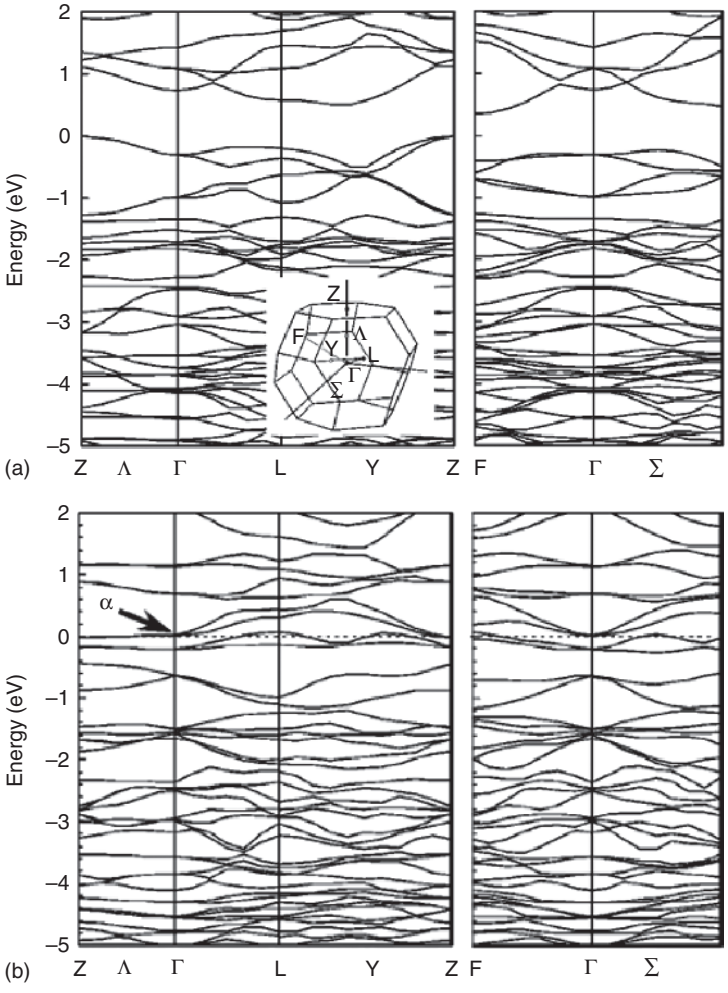

Figure 1.10 Electronic energy bands of the ABC-stacking of rh-phase C_{60} polymer crystals composed of 66/66 bond (a) and 66/65 bond (b) [36].

513 K, the polymer returned to the monomer phase when the temperature was maintained for two hours.

1.2.4 Plasma and EB Irradiation

Polymerization of C_{60} molecules occurs also by applying plasma and irradiating EB on the thin film. Maruyama sublimated C_{60} powder in argon plasma [40]. Owing to the energy of plasma, polymerization occurred. It was confirmed by a shift of $A_g(2)$ peak from 1469 cm^{-1} to a lower frequency; however, the intensity decreased with plasma power and almost diminished after being treated at 50 W. Higher order of merging of the C_{60} molecules such as peanut-shaped inter-C_{60} crosslink structures is proposed in this process.

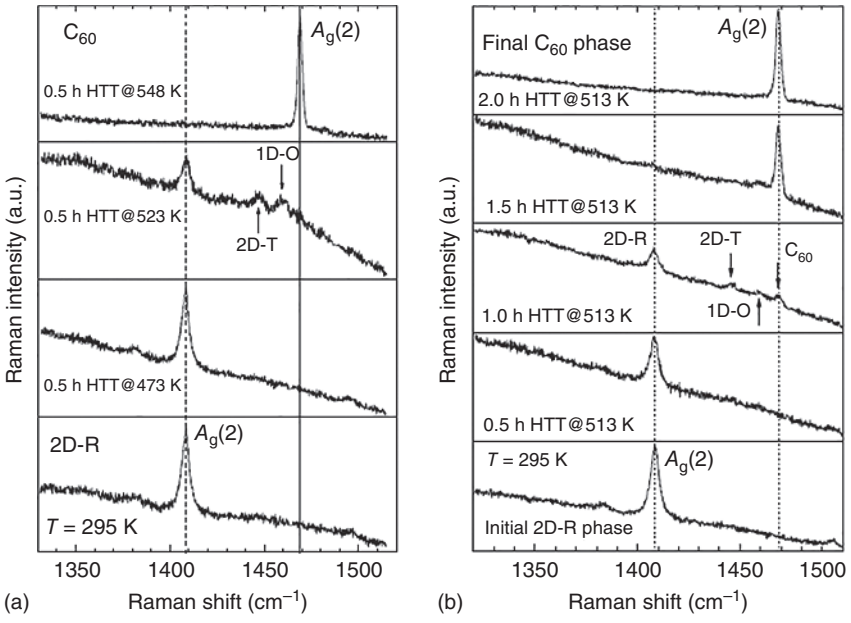

Figure 1.11 Raman spectra of $A_g(2)$ peak in the pure rhombohedral polymer measured at room temperature after heat treatment at various temperatures (a). Time dependence of the peak shift at 513 K (b) [39].

Especially, since such an EB can be focused and irradiated in a selected region, this method is proposed to use C_{60} molecules as a resist material for EB lithography. Tada et al. reported that C_{60} thin film acted as a negative e-beam resist with a sensitivity of 1×10^{-2} C cm^{-2} [41]. Although it is several orders of magnitude worse than the usual resist materials in sensitivity, it shows higher dry-tech durability than conventional novolac resists. However, the solubility in organic solvent becomes almost disappear after in the EB treatment. Therefore, how to remove the polymer in the process is still remained as one of the problems in the practical use.

1.2.5 Low-Energy EB Irradiation

Although sufficient EB irradiation may break a cage of C_{60} fullerene, low-energy EB can provide a different type of C_{60} polymer. The formation of a peanuts-type C_{60} dimer (C_{120} structure) as shown in Figure 1.12a is proposed by Onoe et al. and then a 1D chain of such a structure would be formed by EB irradiation [42]. The intermolecular bonding scheme is different from that of the usual [2+2] cycloaddition reaction. The fusion of adjacent C_{60} molecules via Stone–Wales (S–W) transition is assisted by EB irradiation. Since the S–W transition is not unique, many kinds of allotropes of peanuts-type structures are shown by first principles density functional theory (DFT) calculation with their band structures by Ohno et al. [43]. According to their results, some of the structures do not have a bandgap at the Fermi level and then they may have a metallic property.

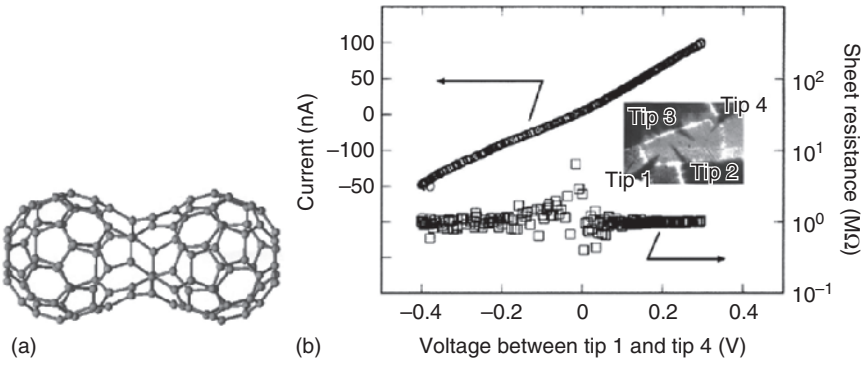

Figure 1.12 (a) Schematic illustration of peanuts-type C_{60} dimer (C_{120} structure). (b) Current–voltage curve and sheet resistance of electron-beam-irradiated sample for 20 hours [42].

Onoe et al. irradiated EB with an acceleration voltage of less than 3 keV on a C_{60} thin film in ultrahigh vacuum conditions. The polymer showed metallic transport properties, and can be explained as a pi-conjugated system. The resistivity of the EB-irradiated sample for 20 hours showed 7 Ω cm by a four-probe method at room temperature. An almost linear current–voltage curve was obtained even in air. No trace of transition into an amorphous phase was observed in the infrared spectra of the sample even after 20 hours of EB irradiation [44]. In order to confirm the electron structure of the polymer around the Fermi energy, they observed *in situ* high-resolution ultraviolet photoemission spectroscopy (UPS). The irradiation time dependence of the UPS spectrum shows increases in the density of states of the HOMO band and monotonically close to the Fermi level as well as the broadening of HOMO peaks with increase in the irradiation time (Figure 1.13). After five hours of irradiation, the density of states exists almost

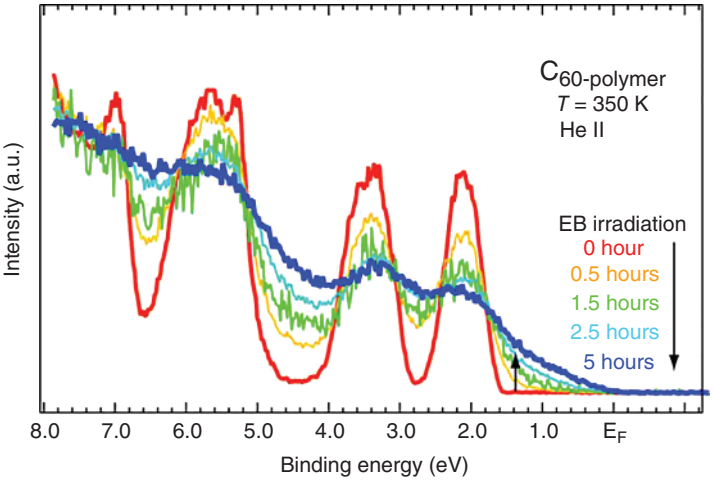

Figure 1.13 Evolution of valence photoelectron spectra of a C_{60} thin film by irradiating with low-energy electron beam as a function of irradiation time [44].

close to the Fermi level. In addition, a finite density of states at the Fermi level has been observed in the UPS spectrum after 12 hours of irradiation, which suggests a metallic property. Unfortunately, the temperature dependence of the resistance of the EB-irradiated sample increased with decreasing temperature, showing a thermal activation-type transport property. This indicates that the system is highly disordered even in the metallic state. However, the activation energy is reported as approximately 100 meV, which is almost half of that of a pristine C_{60} thin film. Therefore, a low-energy EB-irradiated thin film is more conductive than the pristine one. They confirmed that the conductivity can be maintained even in air (Figure 1.12b).

1.3 Summary

Various kinds of polymerization regimes have been studied in C_{60} fullerene. Although C_{60} fullerene thin film and crystal have an fcc structure, one-dimensional or-phase and two-dimensional te- and rh-phases have been confirmed in the polymerized structures. The intermolecular bonding is realized by [2+2] cycloaddition mechanism; therefore, the bonding can be broken by heating it over 573 K and the polymer can reversibly return to the monomer. Such an intermolecular bonding can be realized by photo-irradiation, doping with alkali or alkali earth metals, and plasma pressure application at high temperature. Although the pristine thin film FET shows semiconducting properties, it becomes insulating after exposure to air or EB irradiation. In addition, metallic properties have been observed in a C_{60} polymer synthesized by high pressure and high temperature application. Recently, such a metallic property has been confirmed on C_{60} thin films after sufficient photo-irradiation using optical vortex laser or low-energy electron beam irradiation. Very interesting experimental results have been confirmed and reported individually so far. Combining such unique characteristics, flexible integration circuits or a new class of opto-electric device might be realized by using fullerene molecules.

Acknowledgments

I thank Prof. T. Omatsu, Prof. J. P. Bird, Y. Ochiai, and Prof. T. Kato for the kind support and discussion. This work was supported by the JST-PRESTO program "Molecular technology and creation of new functions" and JSPS KAKENHI Grants No. 24656009.

References

1 Kuroto, H.W., Heath, J.R., O'Brien, C.S. et al. (1985). *Nature* 318: 162.
2 Kraetschmer, W., Lamb, L.D., Fostiropoulos, K., and Huffman, D.R. (1990). *Nature* 347: 354.
3 Hosoya, M., Ichimura, K., Wang, Z.H. et al. (1994). *Phys. Rev. B* 49: 4981.

4 Hora, J., Pánek, P., Navrátil, K. et al. (1996). *Phys. Rev. B* 54: 5106.
5 Mishori, B., Shapira, Y., Belu-Marian, A. et al. (1997). *Chem. Phys. Lett.* 264: 163.
6 Pintschovius, L., Chaplot, S.L., Roth, G., and Heger, G. (1995). *Phys. Rev. Lett.* 75: 2843.
7 Lee, C.H., Yu, G., Kraabel, B. et al. (1994). *Phys. Rev. B* 49: 10572.
8 Hamed, A., Sun, Y.Y., Tao, Y.K. et al. (1993). *Phys. Rev. B* 47: 10873.
9 Rao, A.M., Zhou, P., Wang, K.A. et al. (1993). *Science* 259: 955.
10 Eklund, P.C., Rao, A.M., Zhou, P. et al. (1995). *Thin Solid Films* 257: 185.
11 Pekker, S., Forro, L., Mihaly, L., and Janossy, A. (1994). *Solid State Commun.* 90: 349.
12 Adams, G.B., Page, J.B., Sankey, O.F., and O'Keeffe, M. (1994). *Phys. Rev. B* 50: 17471.
13 Strout, D.L., Murry, R.L., Xu, C.H. et al. (1993). *Chem. Phys. Lett.* 214: 576.
14 Okada, S. and Saito, S. (1997). *Phys. Rev. B* 55: 4039.
15 Paloheimo, J., Isotalo, H., Kastner, J., and Kuzmany, H. (1993). *Synth. Met.* 55–57: 3185.
16 Haddon, R.C., Perel, A.S., Morris, R.C. et al. (1995). *Appl. Phys. Lett.* 67: 121.
17 Li, H., Tee, B., C.-K., Cha, J.J. et al. (2012). *J. Am. Chem.Soc.* 134: 2760.
18 Horiuchi, K., Uchino, S., Nakada, K. et al. (2003). *Physica B* 329–333: 1538.
19 Horiuchi, K., Nakada, S., Uchino, S. et al. (2002). *Appl. Phys. Lett.* 81: 1911.
20 Sze, S.M. and Ng, K.K. (2007). *Physics of Semiconductor Devices*, 3e. Wiley.
21 Horiuchi, K., Uchino, S., Hashii, S. et al. (2004). *Appl. Phys. Lett.* 85: 1987.
22 Zhou, P., Rao, A.M., Wang, K.-A. et al. (1992). *Appl. Phys. Lett.* 50: 2871.
23 Iwasa, Y., Tanoue, K., Mitani, T., and Yagi, T. (1998). *Phys. Rev. B* 58: 16 374.
24 Dzwilewski, A., Wågberg, T., and Edman, L. (2007). *Phys. Rev. B* 75: 75203.
25 Onoe, J., Nakayama, T., Aono, M., and Hara, T. (2004). *J. Appl. Phys.* 96: 443.
26 Aoki, N., Omatsu, T. et al., to be published in elsewhere.
27 (a) Gunnarson, O. (1997). *Rev. Mod. Phys.* 69: 575. (b) Zhao, W.B., Chen, J., Wu, K. et al. (1994). *J. Phys.: Condens. Matter* 6: 631.
28 Xiang, X.-D. et al. (1992). *Science* 256: 1190.
29 Chauvet, O., Oszlanyi, G., Forro, L. et al. (1994). *Phys. Rev. Lett.* 72: 2721.
30 Pakker, S. et al. (1994). *Solid State Comm.* 90: 349.
31 Pekker, S., Janossy, A., Mihaly, L. et al. (1994). *Science* 265: 1077.
32 lwasa, Y., Arima, T., Fleming, R.M. et al. (1994). *Science* 264: 1570.
33 Núñez-Regueiro, M., Marques, L., Hodeau, J.-L. et al. (1995). *Phys. Rev. Lett.* 74: 278.
34 Davydov, V.A., Kashevarova, L.S., Rakhmanina, A.V. et al. (1997). *Carbon* 35: 735.
35 Makarova, T.L., Sundqvist, B., Scharff, P. et al. (2001). *Carbon* 39: 2203.
36 Okada, S. and Oshiyama, A. (2003). *Phys. Rev. B* 68: 235402.
37 Rao, C.N.R., Govindaraj, A., Aiyer, H.N., and Seshadri, R. (1995). *J. Phys. Chem.* 99: 16814.
38 Rao, A.M., Eklund, P.C., Hodeau, J.-L. et al. (1997). *Phys. Rev. B* 55: 4766.
39 Meletov, K.P., Arvanitidis, J., Christofilos, D. et al. (2010). *Cabon* 48: 2974.
40 Maruyama, R. (2007). *J. Molec. Struct.* 10–17: 831.
41 Tada, T. and Kanayama, T. (1997). *J. Photopolymer Sci. and Technol.* 10: 647.

42 Onoe, J., Nakayama, T., Aono, M., and Hara, T. (2003). *Appl. Phys. Lett.* 82: 595.
43 Ohno, K., Noguchi, Y., Ueda, S., and Onoe, J. (2007). *Eur. Phys. D* 43: 137.
44 Onoe, J., Ito, T., and Kimura, S. (2008). *J. Appl. Phys.* 104: 103706.